Effect of Acute High-Intensity Exercise on Rat Myocardium metabolic Profiles. An LC-MS Based Metabolomics Study

Lijun Wu
Shanxi University
Jiayi WANG (2458349847@qq.com)
Shanxi University
Xiuhui Cao
Shanxi University
Yue Tian
Shanxi University
Jia Li
Shanxi University

Research Article

Keywords: Acute high-intensity exercise, Rat myocardium, metabolomics, LC-MS

Posted Date: February 2nd, 2022

DOI: https://doi.org/10.21203/rs.3.rs-1311221/v1

Abstract

Acute high-intensity exercise is a harmful manner associated with a series of myocardial injuries. Metabolism disorder of myocardium is one of the most serious conditions. However, few metabolomics-based studies provide data on the effect of exercise along with myocardial metabolism. Our study aimed to identify metabolic signatures in rat myocardium during acute high-intensity exercise and evaluate their diagnostic potential to sports injuries. SD rats were divided into control group and acute high-intensity exercise group and their myocardium samples were analyzed by LC-MS to explore metabolic alterations of rats' myocardium. This study showed myocardium metabolism clearly differed between the two groups. there were 6 target metabolic pathways and 12 potential metabolic markers for acute high-intensity exercise. Our findings provide an insight that myocardium metabolism during acute high-intensity exercise have distinct disorders in complex lipids and fatty acids. Moreover, an increase of purine degradation products as well as signs of impaired glucose metabolism were observed. However, the amino acid was enhanced, which had a certain protective effect on the myocardium.

Background

Acute high-intensity exercise refers to the increase of cellular energy consumption and changes of substrate energy supply, which leads to a decrease in ATP synthesis efficiency and disorders of material metabolism. This moment, the oxygen supply of tissue decreases, associated with an electron leakage of the mitochondrial respiratory chain, finally inducing oxidative stress damage [1].

Heart is sensitive to exercise intensity. Strenuous sports make myocardium ischemia and hypoxia with systemic metabolic abnormalities and damages. Overtraining has been able to increase the content of angiotensin II and other hormones sharply, which aggravates cardiomyocyte apoptosis and inflammation, causing cardiac dysfunction [2]. Fine material metabolism provides the organism with ATP to ensure the normal operation of cardiomyocytes [3]. Therefore, improving the material metabolism of myocardium is critical to prevent exercise-induced myocardial injury.

Metabolomics is a new approach following genomics, proteomics and transcriptomics, which has the advantages of high throughput, high specificity and high sensitivity. It can capture metabolic states under the specific external stimuli and scans panoramic metabolites to reveal the transition between health and disease [4]. While, the application of metabolomics technology on sports remains unexplored. Here, we analyzed the changes of metabolomics in rat myocardium during acute high-intensity exercise to explain the effect of acute high-intensity exercise on cardiac function from the perspective of material metabolism.

Experimental

Subjects and groups

16 male SD rats at 7 weeks of age (weighing 190–200g , purchased from Beijing vital river laboratory animal technology biotech (Beijing, China), animal license number: SCXK (Beijing) 2016-0006) were randomly divided into a control group (C) and an acute high-intensity exercise group (E), 8 in each group. Raising condition: Light and dark cycled every 12h, free access to tap water and food, the temperature was 26–28°C, the humidity was 50%–60%.

Exercise program

The rats exercised on a three-track rat-special treadmill. On the first day after grouping, group E performed an adaptive exercise, the intensity was 3m/min, the time was 5min, 1 week in total; On the 8th day, Exercise intensity pre-adaptation was conducted with the initial speed of 3m/min, took a break every 3 minutes of exercise and the speed increased by 3m/min after rest until the rat was exhausted (exhaustion standard: rats stayed at the last end of the treadmill, run on the abdomen after an electric shock and returned to the original place within three seconds), repeated 5 times [5]; On the 20th day, the exercise capacity was tested, which based on the Bedford's article [6], the average exhaustion speed was 21m/min (75% VO2max); On the 28th day, did the final acute high-intensity treadmill exercise at a speed of 24m/min, a slope of -16°. The exercise time of each group was 5min, the interval time was 1min, a total of 8 groups.

Samples

After exercise (within 10 minutes), decapitated all rats immediately and stripped the myocardium. The myocardium was washed with ice physiological saline, absorbed dry with filter paper and placed in liquid nitrogen for rapid freezing. After that, stored it at -80°C.

Detection

Reagents and instruments

Acetonitrile (1499230-935, Merckg); Ammonium acetate (70221, Sigma); Ammonia (Fluka). Triple TOF 6600+ mass spectrometer (AB SCIEX); 1290 Infinity LC ultra-high pressure liquid chromatograph (Agilent); ACQUITY UPLC BEH Amide (1.7μm, 2.1 mm×100mm columm) column (Waters); 5430R low temperature high speed centrifuge (Eppendorf).

Sample pretreatment

Thawed each sample at 4°C, weighed 80mg into 2ml EP tubes. added 200ul water to homogenize and vortexed for 1min. Put the pre-cooled 800ul acetonitrile/methanol mixture (1:1, V/V) into the EP tube and put the sample solution in the refrigerator for 1h to remove the sample protein after two low-temperature ultrasonic treatments (30min/time). Later, centrifugated at 4°C and 14000 rcf for 20 minutes, the supernatant was vacuum freeze-dried and stored it at -80°C.

Added 100ul acetonitrile/water (1:1/V: V) mixture and blended thoroughly to reconstitute sample. After centrifugation at 4°C and 14000rcf for 15 minutes, the supernatant was taken for mass spectrometry injection analysis.

The samples were prepared as quality control samples (QC) for testing the instrument and system status. The QC sample was analyzed 4 times at random.

Chromatographic conditions

Put the sample into the autosampler (temperature is 4℃) and added the HILIC chromatographic column. The injection volume was 2ul, the column temperature was 25℃ and the flow rate was 0.3ml/min. Phase A: water+25mmol/L ammonium acetate+25mmol/L ammonia; Phase B: acetonitrile. Gradient elution procedure: 0~0.5min, 95%B; 0.5~7min, 95~65%B; 7~8min, 65~40%B; 8~9min, 40%B; 9~9.1min, 40~95%B; 9.1~12min, 95%B. QC were randomly added to the samples to reduce the signal fluctuations and ensure the data reliability.

Mass spectrometry conditions

Electrospray ionization source setting parameters: ion source gas 1: 60; ion source gas 2: 60; curtain gas: 30; source temperature: 600℃; ionsapary voltage floating: ±5500V. The secondary mass spectrum was obtained through data correlation acquisition in high-sensitivity mode. Related setting parameters: collision energy: 35±15ev; declustering potential: ±60V; candidate ions to monitor per cycle: 6; exclude isotopes: 4Da.

Data processing

Collected data from LC-MS. Used SPSS 24.0 for univariate statistical analysis and SIMCA 14.1 for multivariate statistical analysis based on peak areas data of the detected metabolites. Statistically significant compounds were evaluated by using ROC curve analysis. Made the volcano map and cluster map and Searched Met-PA databases to screen out target metabolic pathways and potential metabolic markers.

Results

QC analysis

The UHPLC-Q-TOF MS ion chromatograms of the QC sample were overlapped and compared (Figure 1, a). the QC sample chromatograms overlapped well, indicating the instrument was in good condition and the experimental data was reliable.

Overall sample Hotellings T2

Overall sample Hotellings T2 analysis was used to detect outliers in this experiment. Here, all samples were within the 99% confidence interval and there were no outliers (Figure 1, b).

Typical metabolic profile

Myocardial samples were detected by LC-MS to obtain typical metabolic spectrums (Figure 2). The contours of the myocardial metabolites between the two groups had changed to different degrees. The differences can be found by further analysis.

PLS-DA analysis results

PLS-DA uses to identify experimental data and predict differences between the two groups. This experiment supervised the data of the two groups after myocardial preconditioning and established a regression model. The model parameters (7 cycles of verification) showed the model establishment was stable and reliable (Table 1). Constructed a PSL-DA model score chart (Figure 3). The positive and negative ion points between group C and group E had a significant separation trend but within the group were more concentrated, indicating the metabolites of the two groups had differences.

Table1 PLS-DA analysis model parameter table

Grouping	Negative ion mode				Positive ion mode			
	A	R^2_X(cum)	R^2_Y(cum)	Q^2(cum)	A	R^2_X(cum)	R^2_Y(cum)	Q^2(cum)
E/C	3	0.477	0.999	0.897	2	0.242	0.995	0.754

Note: A is the number of main components; R^2 is the explanatory rate of model variables to X or Y; Q^2 is the predictive ability of the model; the closer R^2_Y and Q^2 are to 1, the more stable and reliable the model is; the model is stable and reliable when Q^2 is greater than 0.5

OPLS-DA analysis results

OPLS-DA statistical analysis revises the PLS-DA experimental data and enhances the significance of the differences between groups. The model parameters were shown in table 2. In this study, R^2_Y and Q^2 were both greater than 0.5, indicating the two groups had significant differences and the OPLS-DA model is stable and reliable. Constructed the OPLS-DA model score chart (Figure 4). The separation trend of positive and negative ions between the two groups was obvious but the tendency of aggregation within the group was obvious, indicating the metabolites of the two groups had significant differences.

Created 200 models on the basis of OPLS-DA to perform permutation tests on the random sorting of categorical variables Y and determined the R^2 and Q^2 values of the random model (Figure 5). On the same abscissa, the R^2 value was greater than the Q^2 value and can be well separated. The rightmost points of R^2 and Q^2 were both larger than the other points, the leftmost value of Q^2 was less than 0, indicating the model verification of this research had passed, the metabolites of the two groups existed differences and the analysis of PLS-DA, OPLS-DA results was meaningful.

Table 2 OPLS-DA analysis model parameter table

Grouping	Negative ion mode				Positive ion mode			
	A	R^2_X(cum)	R^2_Y(cum)	Q^2(cum)	A	R^2_X(cum)	R^2_Y(cum)	Q^2(cum)
E/C	1+2	0.477	0.999	0.817	1+1	0.242	0.995	0.796

Note: A is the number of main components; R^2 is the explanatory rate of model variables to X or Y; Q^2 is the predictive ability of the model; the closer R^2_Y and Q^2 are to 1, the more stable and reliable the model is; the model is stable and reliable when Q^2 is greater than 0.5

Univariate statistical analysis results

Combined T test and FC analysis to make Volcano Plot (Figure 6). Visually displayed the significantly changed metabolites between the two groups and speed up the screening of potential metabolic markers involved in the pathway. On the basis of $p<0.05$, FC>1.5 or FC<0.67, the substances represented by the red dots in the upper left and upper right corners of the coordinates were the difference metabolites.

Comparison results of different metabolites

The VIP value obtained from OPLS-DA analysis screened the difference metabolites. The T test and FC analysis judged the significance of difference metabolites between the two groups and whether the difference metabolites increased or decreased. VIP>1.0, $p<0.05$, FC>1.5 represented the differential metabolites were significantly increased; VIP>1.0, $p<0.05$, FC<0.67 represented the differential metabolites were significantly decreased. The metabolites of the two groups were screened. It was found there were 32 different metabolites between group C and group E in the positive and negative ion mode (Table 3).

Table 3 Different metabolites and change trend in positive and negative ion mode of E/C group (n=8)

Mode	quantity	Mass-to-charge ratio	Retention time (s)	Differential metabolites	Variation tendency
ESI+	1	120.079	150.693	Tyramine	↓**
ESI+	2	810.599	50.791	1-Stearoyl-2-oleoyl Lecithin (SOPC)	↑**
ESI+	3	496.336	216.480	1-palmitoyl-sn-glyceryl-3-phosphocholine	↑**
ESI+	4	171.004	471.382	Glyceraldehyde 3-phosphate	↑*
ESI+	5	145.049	335.610	L- (-) Sorbitose	↑*
ESI+	6	426.318	225.515	cholic acid	↓*
ESI+	7	123.054	456.870	Nicotinamide	↓*
ESI+	8	400.339	169.317	L-palmitoyl carnitine	↑*
ESI+	9	134.044	449.359	L-Aspartic Acid	↑*
ESI+	10	734.564	175.564	Phosphatidylcholine	↑*
ESI+	11	278.061	472.020	D-glucose 6-phosphate	↑*
ESI+	12	175.119	579.330	L-Arginine	↑*
ESI+	13	127.038	471.296	Larrisic acid	↑*
ESI+	14	109.027	452.725	Quinone	↑*
ESI-	15	175.024	370.209	D-galacturonic acid	↑**
ESI-	16	267.195	68.536	Thapsic acid	↑**
ESI-	17	187.133	102.738	3-hydroxydecanoic acid	↑**
ESI-	18	180.033	124.399	Acamprosate	↑**
ESI-	19	613.137	441.629	Cytidine monophosphate N-acetylneuraminic acid	↑**
ESI-	20	241.082	98.070	Thymidine	↑**
ESI-	21	103.039	188.660	D (-)-β-hydroxybutyric acid	↑**
ESI-	22	125.035	73.774	Thymine	↑**
ESI-	23	111.020	85.016	Uracil	↑**
ESI-	24	295.226	62.648	L-arabinose 1,4-lactone	↑**
ESI-	25	147.029	76.925	D-arabin-1,4-lactone	↑*
ESI-	26	191.016	99.294	D-galactate	↑*

ESI-	27	259.020	500.028	D-mannose 1-phosphate	↑*
ESI-	28	179.055	258.625	D-Mannose	↑*
ESI-	29	227.200	102.618	Myristic acid	↑*
ESI-	30	289.032	462.109	D-ribose 5-phosphate	↑*
ESI-	31	279.231	157.648	Linoleic acid	↑*
ESI-	32	303.231	137.760	Arachidonic acid (peroxide-free)	↑*

Note: * means $p<0.05$ for comparison between the two groups; ** means $p<0.01$ for the comparison between the two groups; ↑ means that the change of the difference is an upward trend; ↓ means that the change of the difference is an upward trend

Hierarchical clustering analysis of differential metabolites

The difference metabolites of myocardial samples between the two groups were analyzed by hierarchical cluster analysis (Figure 7). The red was a significant increase in metabolites, The blue was a significant decrease in metabolites. Here, the color changes of the samples in the same group were relatively concentrated and that of different groups were sharply contrasted, indicating the differences of the myocardial metabolites within the group were small but the differences between the groups were obvious. The selected different metabolites were reliable.

Pathway analysis of target metabolites

MetaboAnalyst 4.0 was used to analyze the differential metabolites between the two groups by Met-PA approach. Imported the data of 32 different metabolites into Pathway Analysis to explore the weight of the metabolic pathways involved (Figure 8). There were 26 metabolic pathways involved during high-intensity exercise (Table 4). Here, Raw $p<0.05$ and Pathway Impact>0.05 were used as the critical point to screen the above-mentioned metabolic pathways. We found there were 6 potential target metabolic pathways that affect the myocardial metabolism of rats during acute high-intensity exercise, namely fructose and mannose metabolism, Linoleic acid metabolism, pyrimidine metabolism, niacin and nicotinamide metabolism, arginine metabolism, amino sugar and nucleotide sugar metabolism (Figure 9).

Table 4 Differential metabolite pathway analysis results obtained through Met-PA

Pathway	Total	Expected	Hits	Raw p	FDR	Impact
Linoleic acid metabolism	5	0.08284	2	0.00282	0.2148	1
Arginine metabolism	14	0.23194	2	0.01365	0.39832	0.07614
Amino sugar and nucleotide sugar metabolism	37	0.61299	3	0.02228	0.39832	0.07043
Niacin and Niacinamide metabolism	15	0.24851	2	0.02473	0.39832	0.1943
Pyrimidine metabolism	39	0.64612	3	0.02963	0.39832	0.17143
Biosynthesis of neomycin, kanamycin and gentamicin	2	0.03314	1	0.02963	0.39832	0
Fructose and mannose metabolism	18	0.29821	2	0.03329	0.39832	0.12422
Biosynthesis of Pantothenic Acid and CoA	19	0.31478	2	0.03937	0.39832	0
Beta-alanine metabolism	21	0.34791	2	0.04664	0.42614	0
Biosynthesis of unsaturated fatty acids	36	0.59642	2	0.1179	0.82529	0
Glycerophospholipid metabolism	36	0.59642	2	0.1179	0.82529	0.11182
Arachidonic acid metabolism	36	0.59642	2	0.1179	0.82529	0.33292
Aminoacyl-tRNA biosynthesis	48	0.79523	2	0.18753	1	0
Alpha-linolenic acid metabolism	13	0.21537	1	0.19592	1	0
Histidine metabolism	16	0.26508	1	0.23559	1	0
Starch and sucrose metabolism	18	0.29821	1	0.26098	1	0.13851
Pentose phosphate pathway	21	0.34791	1	0.29756	1	0.18501
Galactose metabolism	27	0.44732	1	0.36557	1	0
Alanine aspartate and glutamic acid	28	0.46388	1	0.37627	1	0.22356
Inositol phosphate metabolism	30	0.49702	1	0.39716	1	0
Arginine and proline metabolism	38	0.62956	1	0.47419	1	0.05786
Biosynthesis of primary bile acids	46	0.76209	1	0.54172	1	0
Metabolic degradation of fatty	39	0.64612	1	0.48312	1	0
Tyrosine metabolism	42	0.69583	1	0.50907	1	0.02463
Biosynthesis of fatty acids	47	0.77866	1	0.54955	1	0
Purine metabolism	66	1.09342	1	0.67608	1	0.01334

Note: Total is the total number of compounds in the pathway; Expected is the expected value; His is the number of accurate matches in the uploaded marker data; Raw P is the original P value obtained through the analysis of the pathway score map; FDR is the error trigger rate; Impact is obtained through topological analysis Out-of-path influence value

Metabolic markers of rat myocardium

The receiver operating characteristic curve (ROC) evaluated the diagnostic ability of differential metabolites during acute high-intensity exercise. Combined the area value (AUC) and P value (P<0.05) under the ROC curve to screen out the potential metabolism of the above 6 acute high-intensity exercise metabolic pathways. It was Thymine (AUC=1.0), linoleic acid (AUC=0.84), cytidine-phosphate-N-acetylneuraminic acid (AUC=1.0), L-aspartic acid (AUC=0.85), 1-Stearoyl-2-oleoyl lecithin (AUC=1.0), thymidine (AUC=0.93), uracil (AUC=0.89), D-mannose (AUC=0.87), lecithin (AUC=0.95), L-arginine (AUC=0.94), nicotinamide (AUC=0.86), D-mannose, 1-alanine phosphate (AUC=0.91). In this study, these 12 metabolites were regarded as potential markers affecting fatigue metabolism.

Table 5 Potential metabolic markers KEGG ID

Metabolites	KEGG ID	Metabolites	KEGG ID
Linoleic acid	C01595	D-mannose-1-phosphate	C00636
1-stearoyl-2-oleoyl lecithin	C00157	D-Mannose	C00159
Nicotinamide	C00153	Uracil	C00106
L-Aspartic Acid	C00049	L-Arginine	C00062
Thymidine	C00214	Cytidine-phosphate-N-acetylneuraminic acid	C00128
Thymine	C00178	Phosphatidylcholine	C00157

Discussion

Metabolomics studies the metabolic mechanism from the overall metabolite profile. This study used LC-MS to explore the influence of acute high-intensity exercise on rat myocardial metabolism. We found there were 32 different metabolites, participating in 26 metabolic pathways during acute high-intensity exercise. Among them, fructose and mannose metabolism, linoleic acid metabolism, pyrimidine metabolism, niacin and nicotinamide metabolism, arginine metabolism, amino sugar and nucleotide sugar metabolism were the 6 target metabolic pathways during acute high-intensity exercise involved in 12 potential metabolic markers.

Phosphatidyl choline (PC), 1-stearoyl-2-oleoyl lecithin (SOPC) and linoleic acid (LA) participated in the metabolic pathway of linoleic acid (Figure 10.a). After acute exercise, the content of PC in subjects' plasma increased, leading to impaired utilization of cardiac fatty acids and inflammation-mediated

metabolic disorders, which induced heart failure [7]. The reason may be that under the high oxidative stress conditions, PCs were easily transformed into lysophosphatidylcholine (LPC) catalyzed by phospholipase A2 (PLA2). LPC induces the production of inflammatory factors such as TGF-β1, IL-1β, accelerates the apoptosis of cardiomyocytes and promotes the development of coronary heart disease [8]. Lu's study showed the myocardium produced a large amount of free radicals during high-intensity exercise and leaded to the overexpression of PLA2, furthermore, accelerated the production of LPC, which finally induced heart damage [9]. The metabolic process and biological effects of SOPC are consistent with those of PC. Research showed after excessive consumption of red meat, the content of SOPC was high and trimethylamine oxide (TMAO) was produced, which was a risk factor to induce coronary atherosclerosis and cardiovascular diseases [10]. In our study, SOPC and PC in group E increased significantly, indicating acute high-intensity exercise increased the cardiac oxidative stress sharply, possibly producing the lipid peroxidation and toxic substances, damaging the health of myocardium. LA were essential nutrients for organisms, which has the functions of lowering blood pressure and promoting microcirculation [11]. However, patients with diastolic dysfunction were found a significant increase of LA in the neointimal part of the myocardium and atherosclerotic plaques which improved lipid metabolism to provide energy for the heart [12]. Study also showed LA increased when the myocardium is in a pathological state, inducing myocardial hypertrophy through the calcineurin-activated T cell nuclear factor signaling pathway. In addition, the oxidation products of LA can be easily produced because of oxidative stress during acute high-intensity exercise, which causes macrophage apoptosis and induced coronary plaque rupture, thrombus formation or myocardial infarction [13]. In this study, LA in group E was significantly increased, indicating the organism accordingly improved the utilization of myocardium fatty acids during acute high-intensity exercise. However, myocardial ischemia and hypoxia is prone to generate linoleic acid oxidation products or its derivatives, causing heart damage.

D-mannose and D-mannose-1-phosphate participated in the metabolic pathway of fructose and mannose (Figure10.c). D-Mannose exists as a component of mannan in the body, which will be phosphorylated into D-mannose-6-phosphate by hexokinase. Later, a small part is isomerized to form D-mannose-1-phosphate [14]. D-mannose is structurally similar to glucose. When its content in organism is high, glucose transporter will be snatched by D-mannose to produce high levels of D-mannose-6-Phosphoric acid, which disrupts the aerobic oxidation of glucose, accelerates glycolysis and causes abnormal energy supply to the myocardium. These changes will hinder succinate-mediated activation of hypoxia-inducible factors, thereby inhibiting the expression of vascular endothelial growth factor and heme oxygenase 1, reducing angiogenesis and cardiac antioxidant capacity and ultimately leading to heart disease [15]. Study showed D-mannose in type 2 diabetic rats was significantly increased with the risk of myocardial infarction [16]. Ultramarathon runners also been detected high levels of D-mannose in their urine [17]. D-mannose-1-phosphate easily reacts with proteins or lipids to participates in the glycosylation process and generate glycosylation end products (AGEs) [14]. AGEs cause myocardial lipid metabolism disorders, induce atherosclerosis and mediate myocardial chronic inflammation or cell apoptosis through the myeloid differentiation receptor 2/toll-like receptor 4 pathway, which leads to chronic heart failure [18].

Myocardial pressure, corresponding to heart failure, overloaded during high-intensity exercise, which will made material metabolism abnormal and produced more AGEs [19]. In this study, D-mannose and D-mannose 1-phosphate ($p<0.05$) in group E were significantly increased, indicating the aerobic oxidation of glucose in the rat myocardium during acute high-intensity exercise was blocked and the glucose metabolism was disturbed. At this time, cardiovascular regeneration and antioxidant capacity decreased, promoting the production of AGEs and inducing heart failure.

Cytidine-phosphate-N-acetylneuraminic acid (CMP-Neu5Ac), D-mannose-1-phosphate and D-mannose participated in the metabolic pathway of amino sugar and nucleotide sugar (Figure 10.e). CMP-Neu5Ac is the activated form of Neu5Ac, existing as the component of glycolipids and glycoproteins. The two is positively correlated. Neu5Ac is synthesized in the cytoplasm of eukaryotic cells and transferred to the nucleus. It is activated by CMP-Neu5Ac synthase to transfer cytidine monophosphate (CMP) residues from cytidine triphosphate (CTP) and generate CMP-Neu5Ac [20]. Study showed the increase of CMP-Neu5Ac caused cardiomyocyte apoptosis and inflammatory response through Rho/ROCK-JNK/ERK signaling pathway, interfered with lipid metabolism and accelerated the occurrence of atherosclerosis, resulting in myocardial injury [21]. Neu5Ac can also cause myosin light chain phosphorylation and integrin aggregation, increase the permeability of endothelial cells and promote the release of oxidized low-density lipoproteins and inflammatory factors, which destroied the intravascular microenvironment and apoptosis of arterial smooth muscles, finally causing a cardiovascular disease [22]. During high-intensity exercise, myocardium ischemic necrosis increased, which promoted the movement of Neu5Ac in serum to the conjugate in plasma, inducing myocardial injury [23], so the concentration of Neu5AC can represent the level of inflammatory response and be served as a marker for heart diseases. In this study, CMP-Neu5Ac ($p<0.01$) increased significantly in group E, indicating the heart damage during acute high-intensity exercise may be related to the inflammatory reaction of the heart.

Niacinamide and L-aspartic acid (Asp) participated in the metabolic pathway of niacin and niacinamide (Figure 10.b). Niacinamide is the precursor of Coenzyme I (NAD+) and has a significant antioxidant effect [24]. Nicotinamide can increase the bioavailable NO content and up-regulate the expression of forkhead box protein 1 (Foxo1) by activating Silent Information Regulator 1 (SIRT1), thereby enhancing angiogenesis activity, inhibiting cardiomyocyte apoptosis and maintaining cardiovascular health [25]. After excessive exercise, more nutrients were consumed, resulting in myocardial ischemia or hypoxia and a significant decrease in Niacinamide [26]. However, supplementing nicotinamide during exercise will increase the antioxidant enzyme activity of cardiomyocytes and mitochondrial protein, activate autophagy to degrade damaged cell components in a timely manner, maintain the homeostasis of cardiomyocytes and improve the exercise endurance of rats [27]. In this study, nicotinamide in group E ($p<0.05$) decreased significantly, showing acute high-intensity exercise reduced myocardial niacinamide, which easily induces myocardial pathological damage. Asp is an important substrate of gluconeogenesis with the effects of protecting cardiovascular health and promoting fatigue recovery [28]. Study showed Asp can reduce hyperammonemia caused by high-intensity exercise and prolong exercise exhaustion time by promoting muscle glycogen retention, free fatty acid oxidation and gluconeogenesis [29].

Supplementing Asp in repeated cycling sprints can increase the concentrations of glutamic acid, alanine, phenylalanine and total amino acid in blood, reduce the body's latic acid production by generating carbonates and maintain the normal PH value of the blood, thereby alleviating exercise fatigue and enhancing the output power in bicycle sprinting [30]. In this study, Asp ($p<0.05$) in group E increased significantly, indicating during acute high-intensity exercise, the rat myocardium will produce Asp to resist the damage of myocardium by improving the oxidative stress, glucose metabolism and lipid metabolism, thereby protecting heart health to a certain extent.

L-arginine (L-Arg) and L-aspartic acid participated in the metabolic pathway of arginine (Figure 10.f). L-Arg is an essential amino acid in human's body with the functions of detoxification and alleviating fatigue [31]. Research showed L-Arg can produced NO, which dilated blood vessels and increased cardiac blood flow to enhance lung ventilation and maximum oxygen uptake, thereby improving coronary perfusion or cardiomyocyte death during strenuous exercise and maintaining the normal cardiopulmonary function [32]. L-Arg can also promote the phosphorylation of PI3K/Akt and then accelerated the secretion of insulin to regulate the glucose transport process, improved the utilization of glucose and alleviated secondary heart damage in diabetic patients [33]. Exogenous supplementation of L-Arg can reduce the MDA of myocardium, lipid peroxides and free radicals, enhance the activity of antioxidant enzymes and ATPase, thereby reducing heart oxidative stress damage after a one-time continuous downhill running [34]. In this study, L-Arg and Asp ($p<0.05$) in group E increased significantly, indicating during acute high-intensity exercise, the metabolism of amino acid was enhanced, which provided energy for the myocardium and protected the heart.

Uracil, thymidine and thymine participated in the metabolic pathway of pyrimidine (Figure 10.d). The three play an important role in the regulatory functions and energy metabolism. Uracil nucleotides in the venous plasma of patients with myocardial ischemia increased significantly to improve cardiac output, protect the ischemic heart and reduce TNF-a-mediated myocardial apoptosis, which were the important positive inotropic factors and alleviated chronic heart failure [35]. Laitano's research showed during the recovery period after high-intensity running wheel training, the level of uracil in the myocardium of mice was significantly increased, which was essential for myocardial repair after strenuous exercise [36]. Study showed the plasma thymine in mice with acute myocardial ischemia increased significantly and the expansion of thymine was closely related to the risk of heart disease [37]. Peng's research showed a significant decrease in thymidine in rats' serum can be used as a biomarker of early acute myocardial infarction [38]. After strenuous exercise, the increase of thymine in rats' serum had been confirmed and it will induce cardiac ischemia damage. Thymidine supplementation can promote the regeneration of rat myocardial cells, provide energy for the heart and improve anti-fatigue ability [39]. In this study, thymine ($p<0.01$) in group E increased significantly, indicating during acute high-intensity exercise, the myocardium was in an ischemic state and the heart may have pathological changes. At this time, uracil and thymidine ($p<0.01$) in myocardium increased which can improve cardiac function.

Conclusion

In this study, we found compared with the control, rat myocardium acute high-intensity exercise had 32 different metabolites and 12 potential metabolic markers which participated in 6 target metabolic pathways by LC-MS and metabolic pathway analysis. Cardiac dysfunction caused by acute high-intensity exercise may be related to myocardial lipid peroxidation, lipid and glucose metabolism disorders. At this moment, the increase of amino acid and nucleotide metabolism in organism can speed up the repair of damaged myocardium and provide energy for myocardium to maintain the normal physiological function of heart. Therefore, improving myocardial material metabolism may be an important target for the treatment of heart disease.

Declarations

Author contributions

L-JW: First author, Providing the funding to this research, Revising the manuscript and confirmation of final version to be published and Submitted manuscript. J-YW: Corresponding author, Substantial contributions to conception and design, performed sample collection and the data analysis, revising the manuscript and confirmation of final version to be published. X-HC: Revising the manuscript. YT: Substantial contributions to conception and design. JL: data analysis.

Ethics approval and consent to participate

This experiment was approved by the ethics committee of Shanxi University (No. SXULL2020064).

Acknowledgement

The authors thank those who contributed to the development of this research.

Funding

This study was supported by the Natural Science Foundation of Shanxi Province (No.:201601D102074) and Shanxi Provincial Key Research and Development Project (No.:201803D31030)

Conflict of interest

The authors declare no conflict of interest.

References

[1] Heinonen I, Sorop O, de Beer V J, et al. What can we learn about treating heart failure from the heart's response to acute exercise? Focus on the coronary microcirculation[J]. Journal of Applied Physiology, 2015, 119(8): 934-943.

[2] McCullough P A, Chinnaiyan K M, Gallagher M J, et al. Changes in renal markers and acute kidney injury after marathon running[J]. Nephrology, 2011, 16(2): 194-199.

[3] Starnes J W, Parry T L, O'Neal S K, et al. Exercise-induced alterations in skeletal muscle, heart, liver, and serum metabolome identified by non-targeted metabolomics analysis[J]. Metabolites, 2017, 7(3): 40.

[4] Oliver S G, Winson M K, Kell D B, et al. Systematic functional analysis of the yeast genome[J]. Trends in biotechnology, 1998, 16(9): 373-378.

[5] Chaves F M, Baptista I L, Simabuco F M, et al. High-intensity-exercise-induced intestinal damage is protected by fermented milk supplemented with whey protein, probiotic and pomegranate (Punica granatum L.) [J]. British Journal of Nutrition, 2018, 119(8): 896-909.

[6] Bedford T G, Tipton C M, Wilson N C, et al. Maximum oxygen consumption of rats and its changes with various experimental procedures[J]. Journal of Applied Physiology, 1979, 47(6): 1278-1283.

[7] Kraenkel N, Koc A, Kaczmarek S, et al. Immune-metabolome response to an acute exercise exertion reveals dysfunctional metabolic recovery in heart failure[J]. European Journal of Preventive Cardiology, 2021, 28(Supplement_1): zwab061. 012.

[8] Paapstel K, Kals J, Eha J, et al. Inverse relations of serum phosphatidylcholines and lysophosphatidylcholines with vascular damage and heart rate in patients with atherosclerosis[J]. Nutrition, Metabolism and Cardiovascular Diseases, 2018, 28(1): 44-52.

[9] Lu Z, Xu Y, Song Y, et al. A Mixed Comparisons of Different Intensities and Types of Physical Exercise in Patients with Diseases Related to Oxidative Stress: A Systematic Review and Network Meta-Analysis[J]. Frontiers in Physiology, 2021, 12.

[10] Iglesias-Carres L, Hughes M D, Steele C N, et al. Use of dietary phytochemicals for inhibition of trimethylamine N-oxide formation[J]. The Journal of Nutritional Biochemistry, 2021: 108600.

[11] Cabout M, Alssema M, Nijpels G, et al. Circulating linoleic acid and alpha-linolenic acid and glucose metabolism: the Hoorn Study [J]. European journal of nutrition, 2017, 56(6): 2171-2180.

[19] Fatima T, Hashmi S, Iqbal A, et al. Untargeted metabolomic analysis of coronary artery disease patients with diastolic dysfunction show disturbed oxidative pathway[J]. Metabolomics, 2019, 15(7): 1-12.

[13] Bannehr M, Löhr L, Gelep J, et al. Linoleic acid metabolite DiHOME decreases post-ischemic cardiac recovery in murine hearts[J]. Cardiovascular toxicology, 2019, 19(4): 365-371.

[14] Torretta S, Scagliola A, Ricci L, et al. D-mannose suppresses macrophage IL-1β production[J]. Nature communications, 2020, 11(1): 1-12.

[15] Balogh V, MacAskill M G, Hadoke P W F, et al. Positron Emission Tomography Techniques to Measure Active Inflammation, Fibrosis and Angiogenesis: Potential for Non-invasive Imaging of Hypertensive Heart Failure[J]. Frontiers in Cardiovascular Medicine, 2021, 8.

[16] Ferrannini E, Marx N, Andreini D, et al. Mannose as a biomarker of coronary artery disease: Angiographic evidence and clinical significance[J]. International journal of cardiology, 2021.

[17] König S, Jockenhöfer C, Billich C, et al. Long distance running–Can bioprofiling predict success in endurance athletes[J]. Medical Hypotheses, 2021, 146: 110474.

[18] Yaru C, Xiumei C, Xiangming W, et al. Correlation analysis of APOE gene polymorphism and advanced glycation end products with coronary heart disease in the elderly[J]. Journal of Nanjing Medical University, 2016, 41(6):908-911.

[19] Tijardović M, Marijančević D, Bok D, et al. Intense physical exercise induces an anti-inflammatory change in IgG N-glycosylation profile[J]. Frontiers in physiology, 2019, 10: 1522.

[20] Traving C, Schauer R. Structure, function and metabolism of sialic acids[J]. Cellular and Molecular Life Sciences CMLS, 1998, 54(12): 1330-1349.

[21] Zhang C, Chen J, Liu Y, et al. Sialic acid metabolism as a potential therapeutic target of atherosclerosis[J]. Lipids in health and disease, 2019, 18(1): 1-11.

[22] Qi W, Qingwu S. Metabolic pathway and harm of N-glycolylneuraminic acid in red meat in human body[J]. Food Research and Development, 2019, 40(8): 7-13.

[23] Okerblom J, Fletes W, Patel H H, et al. Human-like Cmah inactivation in mice increases running endurance and decreases muscle fatigability: implications for human evolution[J]. Proceedings of the Royal Society B: Biological Sciences, 2018, 285(1886): 20181656.

[24] Nadeeshani H, Li J, Ying T, et al. Nicotinamide Mononucleotide (NMN) as an Anti-Aging Health Product-Promises and Safety Concerns[J]. Journal of Advanced Research, 2021.

[25] Jafari-Azad A, Hosseini L, Rajabi M, et al. Nicotinamide mononucleotide and melatonin counteract myocardial ischemia-reperfusion injury by activating SIRT3/FOXO1 and reducing apoptosis in aged male rats[J]. Molecular Biology Reports, 2021, 48(4): 3089-3096.

[26] Bester R, Stander Z, Mason S, et al. Characterizing Marathon-Induced Metabolic Changes Using 1H-NMR Metabolomics[J]. Metabolites, 2021, 11(10): 656.

[27] Li W, Zhu L, Ruan Z B, et al. Nicotinamide protects chronic hypoxic myocardial cells through regulating mTOR pathway and inducing autophagy[J]. Eur Rev Med Pharmacol Sci, 2019, 23(12): 5503-5511.

[28] Ritterhoff J, Young S, Villet O, et al. Metabolic remodeling promotes cardiac hypertrophy by directing glucose to aspartate biosynthesis[J]. Circulation research, 2020, 126(2): 182-196.

[29] Farney T M, MacLellan M J, Hearon C M, et al. The effect of aspartate and sodium bicarbonate supplementation on muscle contractile properties among trained men[J]. The Journal of Strength & Conditioning Research, 2020, 34(3): 763-770.

[30] Yamaguchi K, Hayashi N, Sumi D, et al. Sodium L-Aspartate Supplementation Improves Repeated Cycling Sprint Performance: 846[J]. Medicine & Science in Sports & Exercise, 2021, 53(8S): 282.

[31] Popolo A, Adesso S, Pinto A, et al. L-Arginine and its metabolites in kidney and cardiovascular disease[J]. Amino Acids, 2014, 46(10): 2271-2286.

[32] Rezaei S, Gholamalizadeh M, Tabrizi R, et al. The effect of L-arginine supplementation on maximal oxygen uptake: A systematic review and meta-analysis[J]. Physiological Reports, 2021, 9(3): e14739.

[33] Costa G, Shushanof M, Bouskela E, et al. Oral L-Arginine (5 g/day) for 14 Days Improves Microcirculatory Function in Healthy Young Women and Healthy and Type 2 Diabetes Mellitus Elderly Women[J]. Journal of Vascular Research, 2021: 1-10.

[34] Lee N K L, MacLean H E. Polyamines, androgens, and skeletal muscle hypertrophy[J]. Journal of cellular physiology, 2011, 226(6): 1453-1460.

[35] Mazzola A, Amoruso E, Beltrami E, et al. Opposite effects of uracil and adenine nucleotides on the survival of murine cardiomyocytes[J]. Journal of cellular and molecular medicine, 2008, 12(2): 522-536.

[36] Laitano O, Garcia C K, Mattingly A J, et al. Delayed metabolic dysfunction in myocardium following exertional heat stroke in mice[J]. The Journal of physiology, 2020, 598(5): 967-985.

[37] Lai Q, Yuan G, Wang H, et al. Exploring the protective effects of schizandrol a in acute myocardial ischemia mice by comprehensive metabolomics profiling integrated with molecular mechanism studies[J]. Acta Pharmacologica Sinica, 2020, 41(8): 1058-1072.

[38] Jiang P, Dai W, Yan S, et al. Biomarkers in the early period of acute myocardial infarction in rat serum and protective effects of Shexiang Baoxin Pill using a metabolomic method[J]. Journal of ethnopharmacology, 2011, 138(2): 530-536.

[39] Fiuza-Luces C, Santos-Lozano A, Joyner M, et al. Exercise benefits in cardiovascular disease: beyond attenuation of traditional risk factors[J]. Nature Reviews Cardiology, 2018, 15(12): 731-743.

Figures

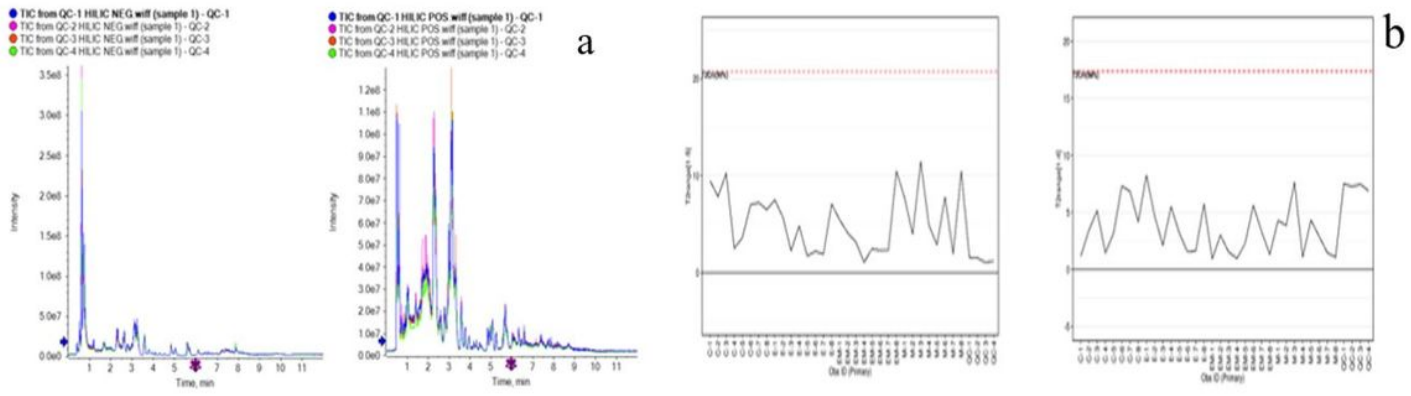

Figure 1

(a) Overlapping TIC spectra of negative and positive ion modes of QC samples; (b) Hotellings T2 diagram in negative and positive ion mode of the sample

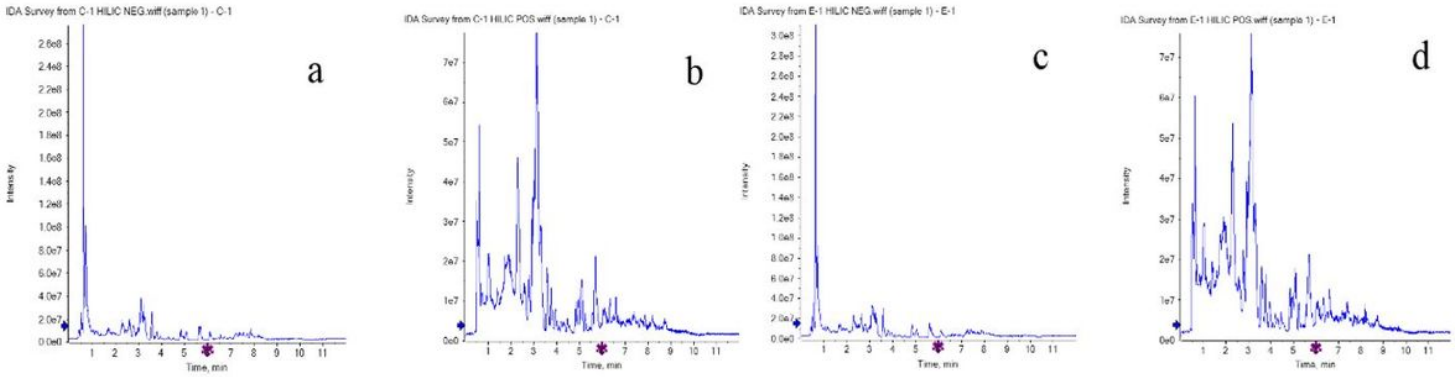

Figure 2

The total ion current diagram of typical metabolites in a myocardial sample. (a) Group C negative ion current diagram; (b) Group C positive ion current diagram; (c) Group E negative ion current diagram; (d) Group E positive ion current diagram

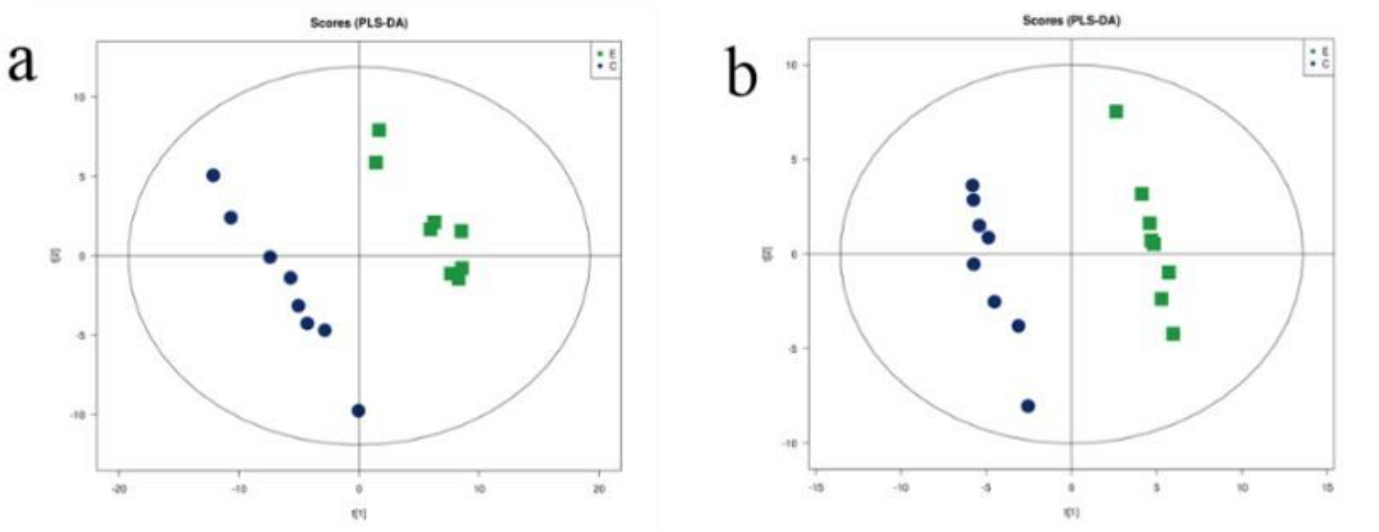

Figure 3

PLS-DA score chart of myocardial samples in positive and negative ion mode. (a) negative ions in group C/E; (b) positive ions in group C/E.

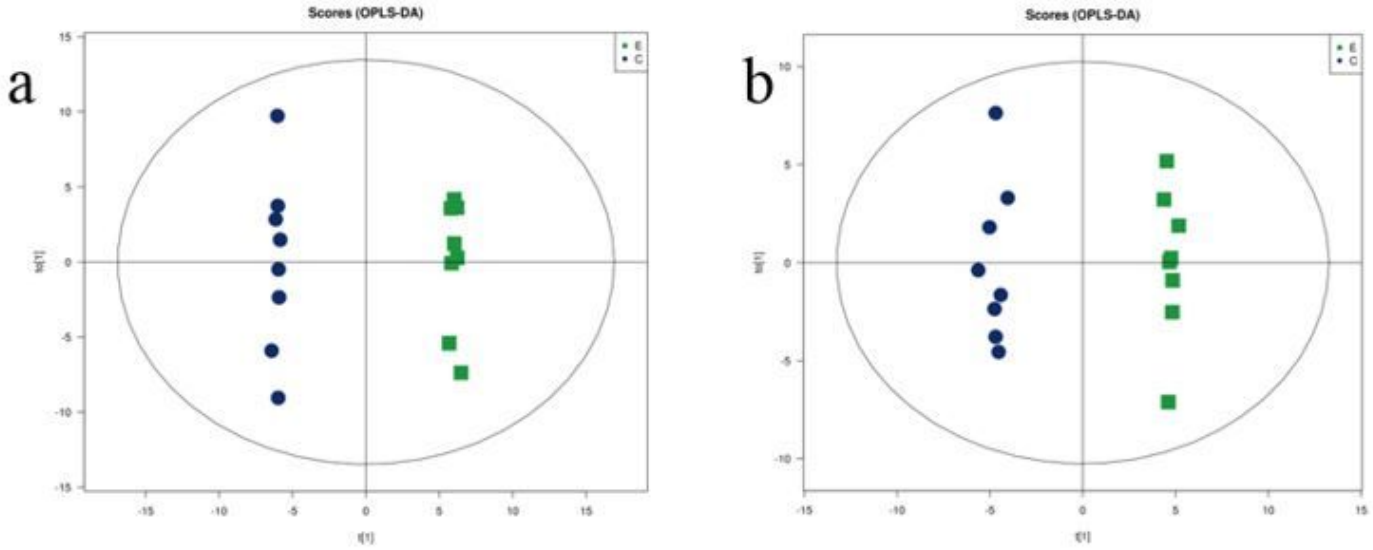

Figure 4

OPLS-DA diagram of myocardial sample positive and negative ions. (a) negative ions in C/E group; (b) positive ions in C/E group.

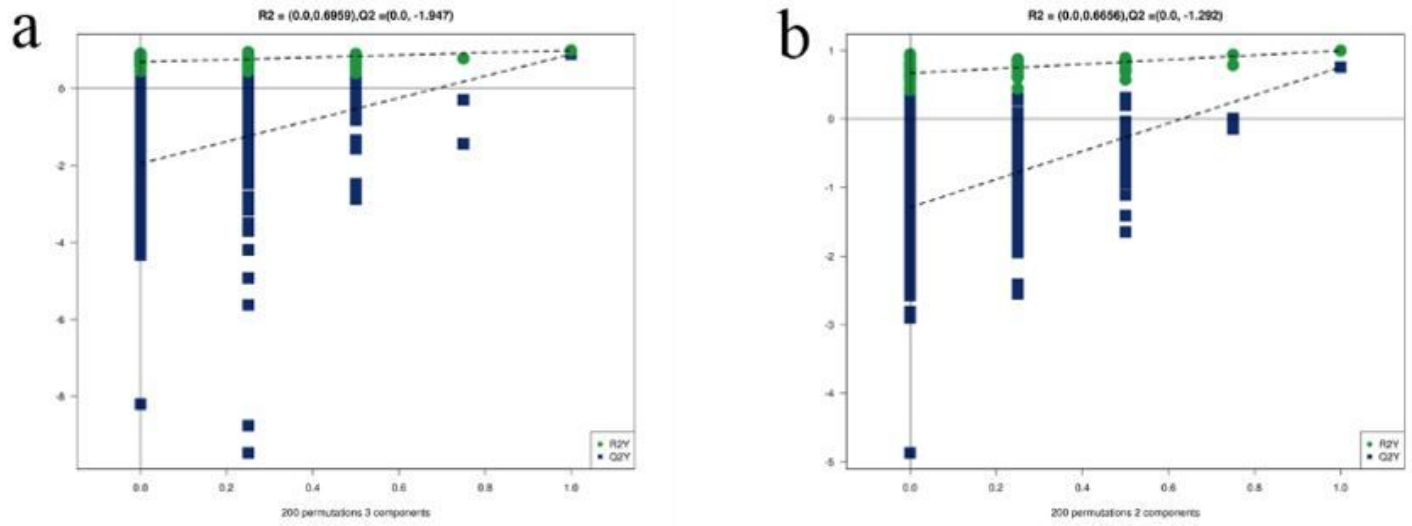

Figure 5

OPLS-DA model replacement test diagram of myocardial sample. (a) E/C group negative ions; (b) E/C group positive ions

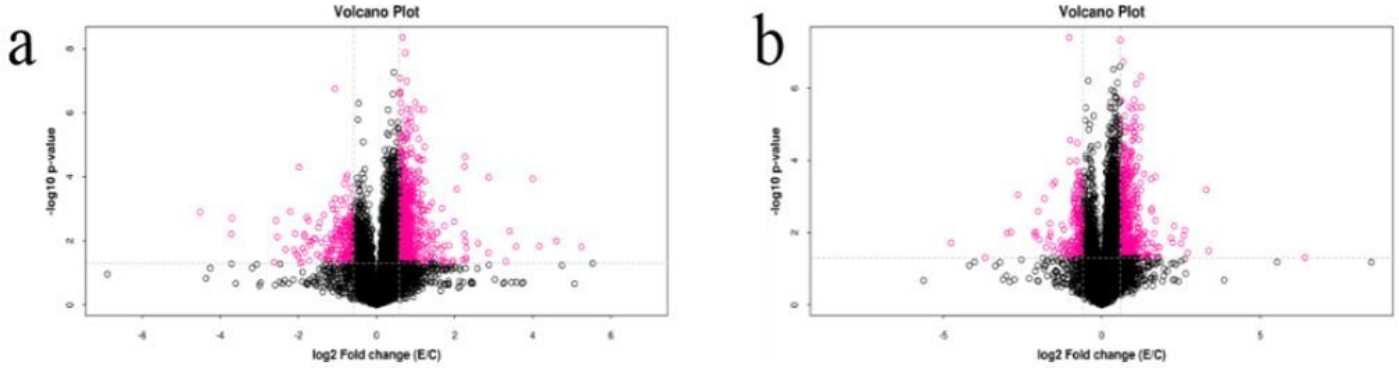

Figure 6

The volcano diagram of the positive and negative ion mode of the myocardial sample. (a) C/E group negative ions; (b) C/E group positive ions

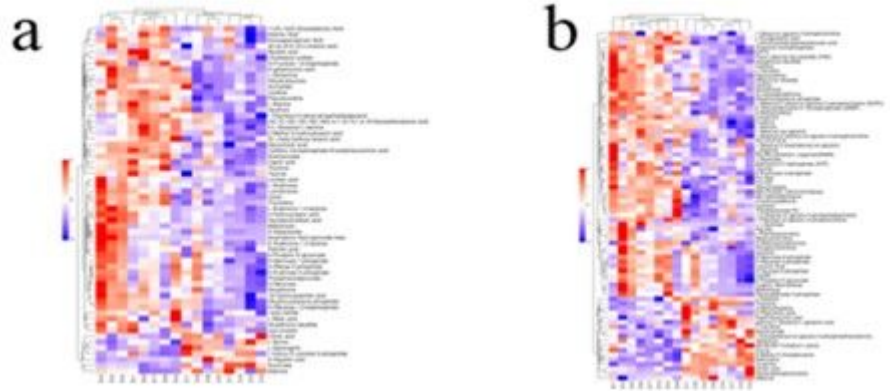

Figure 7

Metabolite hierarchical clustering of significant differences in positive and negative ion patterns in myocardial samples. (a) E/C group negative ions; (b) E/C group positive ions

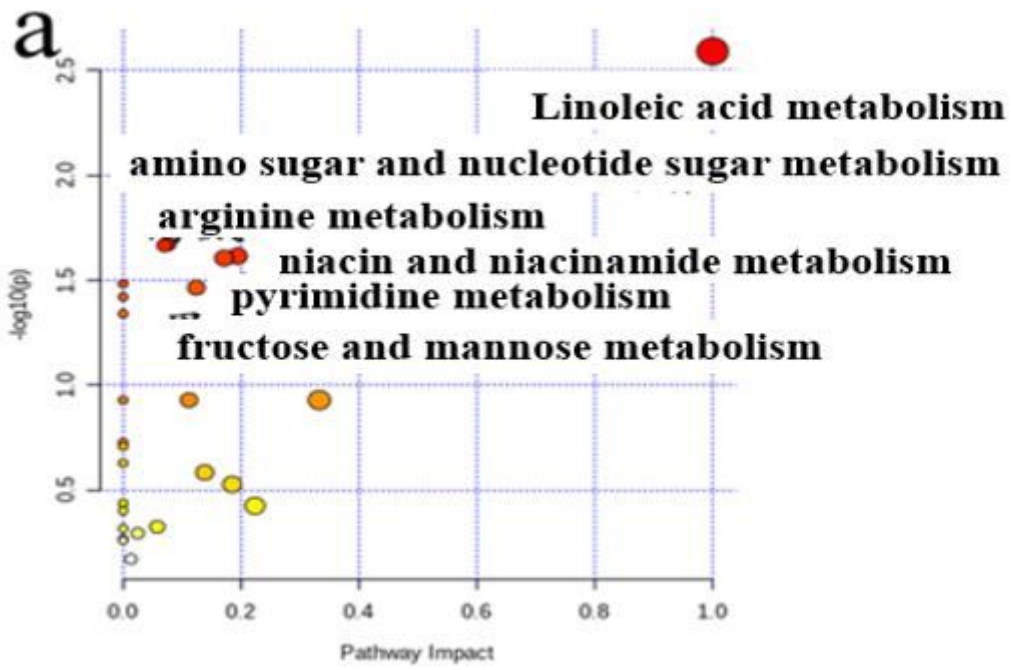

Figure 8

Acute high-intensity exercise metabolic pathways constructed by MetPA database.

Note: The abscissa pathway impact is the importance value of the metabolic pathway obtained by topological analysis, and the ordinate -logP is the significance level of the metabolic pathway enrichment analysis; the greater the pathway impact and -logP value are, the higher the correlation of the metabolic differences between different groups is, the bigger the circle is.

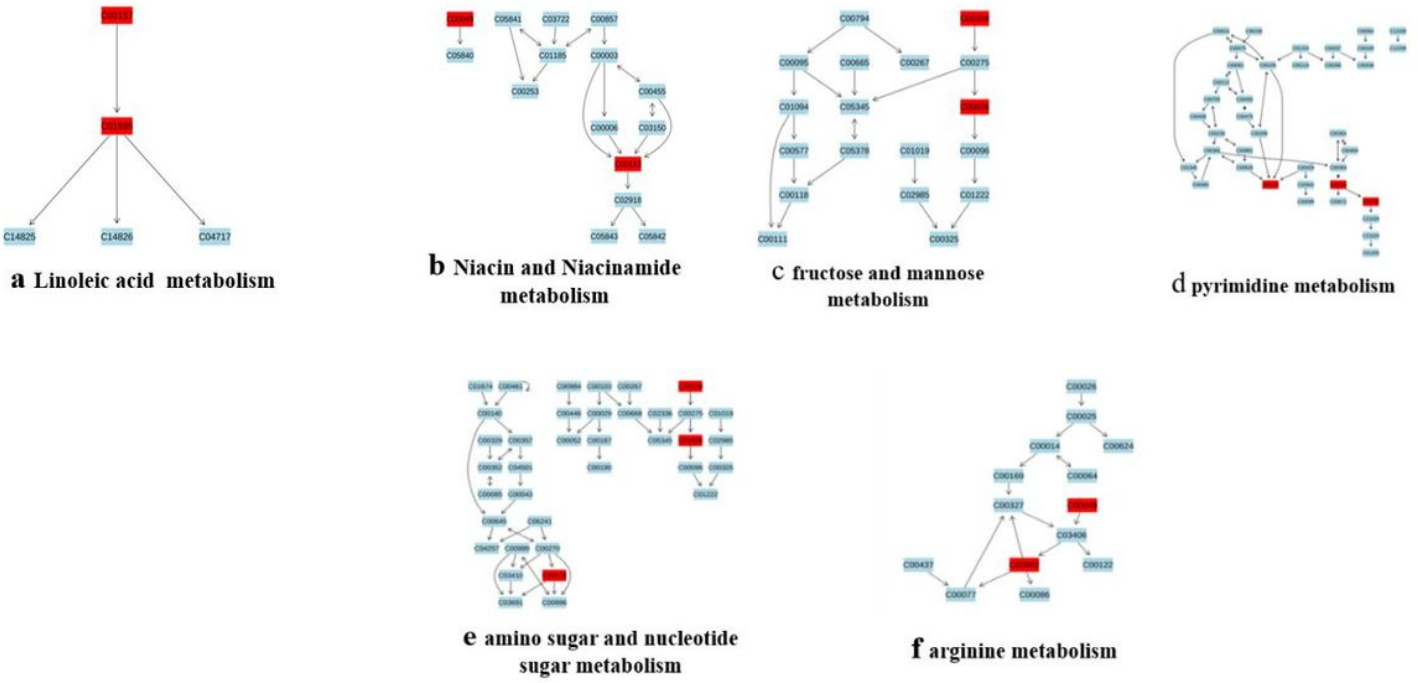

Figure 9

Metabolic pathways involved in differential metabolites. Red is the potential marker of the pathway involved in this study; Blue is not in the metabolites of this study